Cell

Oligodendrocyte-Encoded *HIF* Function Couples Postnatal Myelination and White Matter Angiogenesis

Tracy J. Yuen,[1,6] John C. Silbereis,[1,2,6] Amelie Griveau,[1] Sandra M. Chang,[1] Richard Daneman,[3] Stephen P.J. Fancy,[1] Hengameh Zahed,[1,4] Emin Maltepe,[5] and David H. Rowitch[1,5,*]

[1]Department of Pediatrics, Eli and Edythe Broad Institute for Stem Cell Research and Regeneration Medicine and Howard Hughes Medical Institute

[2]Neuroscience Graduate Program

[3]Department of Anatomy

[4]Medical Science Training Program

[5]Division of Neonatology

University of California, San Francisco, 513 Parnassus Avenue, San Francisco, CA 94143, USA

[6]Co-first author

*Correspondence: rowitchd@peds.ucsf.edu

http://dx.doi.org/10.1016/j.cell.2014.04.052

SUMMARY

Myelin sheaths provide critical functional and trophic support for axons in white matter tracts of the brain. Oligodendrocyte precursor cells (OPCs) have extraordinary metabolic requirements during development as they differentiate to produce multiple myelin segments, implying that they must first secure adequate access to blood supply. However, mechanisms that coordinate myelination and angiogenesis are unclear. Here, we show that oxygen tension, mediated by OPC-encoded *hypoxia-inducible factor* (*HIF*) function, is an essential regulator of postnatal myelination. Constitutive HIF1/2α stabilization resulted in OPC maturation arrest through autocrine activation of canonical *Wnt7a/7b*. Surprisingly, such OPCs also show paracrine activity that induces excessive postnatal white matter angiogenesis in vivo and directly stimulates endothelial cell proliferation in vitro. Conversely, OPC-specific *HIF1/2α* loss of function leads to insufficient angiogenesis in corpus callosum and catastrophic axon loss. These findings indicate that OPC-intrinsic HIF signaling couples postnatal white matter angiogenesis, axon integrity, and the onset of myelination in mammalian forebrain.

INTRODUCTION

Oligodendrocytes (OLs) are the myelinating cells of the central nervous system (CNS). Myelination enables rapid transmission of action potentials through saltatory conduction (Bradl and Lassmann, 2010), and OLs provide trophic support and maintain axon integrity (Fünfschilling et al., 2012; Harris and Attwell, 2012; Lee et al., 2012; Rinholm et al., 2011). Developing oligodendrocyte precursor cells (OPCs) undergo as much as a 6,500-fold increase in membrane area to provide myelin segments to multiple axons (Baron and Hoekstra, 2010; Chong et al., 2012), a process that entails extraordinary metabolic demands (Chrast et al., 2011; Harris and Attwell, 2012; Nave, 2010). Thus, OLs and OPCs require access to a rich vascular supply for nutritive and oxidative substrates. However, OLs are not known to regulate angiogenesis, and molecular mechanisms that might couple the timing of myelination to adequate blood supply during postnatal brain development are unknown.

Hypoxia-inducible factors (HIFs) are transcriptional mediators of the cellular response to hypoxia (Majmundar et al., 2010; Semenza, 2012), comprising a heterodimeric complex of an oxygen-sensitive subunit (HIF1α or HIF2α) with a constitutive subunit (HIF1β or HIF2β) (Hirose et al., 1996; Wang et al., 1995). In normoxic conditions, prolyl hydroxylase (PHD1–PHD3) and von Hippel Lindau (VHL) target HIF1/2α for proteosomal degradation (Ivan et al., 2001; Jaakkola et al., 2001). Conversely, during hypoxia, stabilized HIF1/2α proteins bind HIF1β and translocate to the nucleus to activate gene targets by binding *cis*-acting motifs called hypoxia response elements (HREs) (Mazumdar et al., 2010; Patel and Simon, 2008).

Previous studies show that *Wnt7a/7b* function in embryonic neural precursors is essential for embryonic CNS angiogenesis (Daneman et al., 2009; Stenman et al., 2008). During development, the Wnt pathway is required for maturation of CNS blood vessels and the blood-brain barrier (Liebner et al., 2008; Wang et al., 2012; Ye et al., 2009b), a process that involves vascular investment by pericytes and astrocytic end-feet (Daneman et al., 2010; Janzer and Raff, 1987). Robust CNS angiogenesis persists until postnatal day (P) 10 in mice, which coincides with myelination onset in the corpus callosum (Harb et al., 2013). The most active period of myelination in the postnatal human brain occurs during the first year of life, which correlates with increasing levels

of blood flow and O_2 (Franceschini et al., 2007; Kinney et al., 1988; Miller et al., 2012). Conversely, postnatal hypoxia results in delayed myelination (Ment et al., 1998; Silbereis et al., 2010; Tan et al., 2005; Weiss et al., 2004), in part through activation of Wnt signaling, an inhibitor of OL differentiation (Fancy et al., 2011a, 2011b; Ye et al., 2009a).

To better define molecular pathways that could integrate myelination and vascular supply, we hypothesized that oxygen levels directly regulate the differentiation of OLs. Here, we show that OPC *HIF1/2α* activity inhibits myelination by inducing autocrine *Wnt7a/7b* signaling, which also has a novel paracrine role to promote Wnt-dependent vessel growth into developing postnatal white matter tracts. Although constitutive *HIF* activation in OPCs caused striking hypervascularization throughout the brain, loss of OPC-encoded *HIF1/2α* function resulted in catastrophic loss of corpus callosum axons commencing at P4, when robust angiogenesis is taking place. Our findings establish a HIF (and, by extension, oxygen) -dependent mechanism that is critical to precisely time the onset of myelination to environmental conditions that can adequately support the associated metabolic demands. Moreover, we show an unexpected role for OPCs as critical regulators of angiogenesis in the postnatal brain.

RESULTS

Oxygen Levels and Cell-Intrinsic *VHL* Function Regulate OPC Differentiation and Myelination

In mice, postnatal myelination in the corpus callosum and cerebellar white matter is initiated at about P7–P9 and peaks at P15–P21 (Tessitore and Brunjes, 1988). As shown (Figures 1A, 1B, and S1A–S1C available online), chronic exposure of neonatal mice to mild hypoxia (10% FiO_2) from P3–P11 resulted in hypomyelination and delayed OPC differentiation without altering total OL lineage numbers (Olig2+). This was indicated by reduced expression of myelin basic protein (MBP) and cells expressing the mature lineage-specific marker CC1 (a.k.a., adenomatous polyposis coli, APC), which is consistent with previous findings (Weiss et al., 2004). Under such hypoxic conditions, we observed stabilized HIF1α proteins in white matter lysates and Olig2+ OPCs (Figures 1B and S1D).

We next examined effects of cell-intrinsic HIF stabilization in OPCs. We targeted conditional knockout (KO) of a floxed *VHL* allele (Rankin et al., 2005) through intercrosses with *Sox10-cre* (Stolt et al., 2006), *Olig1-cre* (Lu et al., 2002), or tamoxifen-inducible *Plp-creERT2* (Doerflinger et al., 2003) transgenic mice. As shown (Figure 1B), OPC-specific *VHL* conditional KO by *Sox10-cre* resulted in HIF1α stabilization and severe OPC maturation arrest. We observed hypomyelination throughout the brain of *Sox10-cre*, *VHL*(*fl/fl*) mice (Figures 1B and S1C), which displayed tremor, ataxia, and failure to survive past weaning age (P21). It is possible that lethality resulted from *VHL* loss of function in the peripheral nervous system, which is also targeted by *Sox10-cre* (Stolt et al., 2006). However, *Olig1-cre*, *VHL*(*fl/fl*) mice showed a similar phenotype of hypomyelination and reduced viability past P10 (Figure S1E; data not shown). Together, these findings indicate that cell-intrinsic *VHL* function phenocopies the effects of hypoxia and is required for OPC maturation and myelination.

To further verify that effects of hypoxia on the OL lineage were direct, we purified OPCs by immunopanning from the neonatal brain for in vitro studies (Emery and Dugas, 2013). As shown (Figures 1C and S1F–S1J), exposure to 2% oxygen or treatment with the HIF-stabilizing agent dimethyloxalylglycine (DMOG) inhibited OPC maturation and myelin gene expression (*MAG*, *MBP*, and *CNPase*). We found similar results in OPCs isolated from *Plp-creERT2*, *VHL*(*fl/fl*) mice following treatment with tamoxifen (Figure 1C). These findings show direct effects of oxygen levels on OPCs and indicate that cell-autonomous HIF signaling causes maturation arrest.

Hypoxic Effects on OPCs Are Mediated by *HIF1/2α* Function

We next determined whether *HIF1/2α* function is required for hypoxia-induced hypomyelination. We crossed conditional *HIF1α*(*fl/fl*) and *HIF2α*(*fl/fl*) mutants to compound homozygosity (hereafter called *HIF1/2α*(*fl/fl*)) with *Plp-creERT2* (Doerflinger et al., 2003). Given dramatic hypomyelination observed in the cerebellar white matter of *Sox10-cre*, *VHL*(*fl/fl*) mice (Figure S1C), we utilized a cerebellar explant culture assay suitable to quantify changes in postnatal myelination and compact myelin paranode formation (Fancy et al., 2011b; Yuen et al., 2013). We generated cerebellar explants from P0–P1 transgenic mice and added tamoxifen (which did not affect survival) to induce acute Cre-mediated excision of *HIF1/2α* in OLs (Figures 2A and S2A). Although the *Plp-creERT2* allele has been shown to have variable activity in vivo (Doerflinger et al., 2003), we observed about 85% of Olig2+ cells expressed a conditional (floxed) GFP reporter (Figure S2B). Subsequently, cultures were exposed to hypoxia (2% FiO_2) for 24 hr and maintained for 12 days prior to analysis. As shown (Figures 2B–2D and S2C), hypoxia and subsequent *HIF* activation inhibited myelination and OPC differentiation in wild-type cerebella, as shown by MBP staining, as well as the ratio of Caspr paranode staining to NFH^+ axons, and the increased ratio of Nkx2.2 (immature OPCs)/Olig2 (total OLs) double-positive cells (Fancy et al., 2011b). However, as shown (Figures 2B–2F and S2C–S2E), the degree of hypomyelination and OPC differentiation block was significantly reduced by deletion of *HIF1/2α*. Thus, hypoxia-induced hypomyelination and maturation arrest requires intact *HIF* function within OPCs (Figure 2G). Our findings do not rule out a role of other pathways (e.g., apoptosis-inducing factor and AMP-activated protein kinase [Hardie et al., 2012; Joza et al., 2009]) in hypoxic regulation of OPCs.

HIF Stabilization in OPCs Activates Canonical Wnt Signaling

In OPCs, canonical Wnt signaling functions as a potent inhibitor of maturation (Fancy et al., 2009). We have further reported that hypoxia-induced hypomyelination in vitro can be normalized by treatment with XAV939 (Fancy et al., 2011b; Huang et al., 2009) (Figure 3A).

To determine whether HIF signaling activates the Wnt pathway in white matter in vivo, we performed western blot analysis of P11 corpus callosum lysates from wild-type mice exposed to chronic hypoxia and normoxic *Sox10-cre*, *VHL*(*fl/fl*) conditional KOs. As shown (Figures 3B and S3A), we observed upregulation

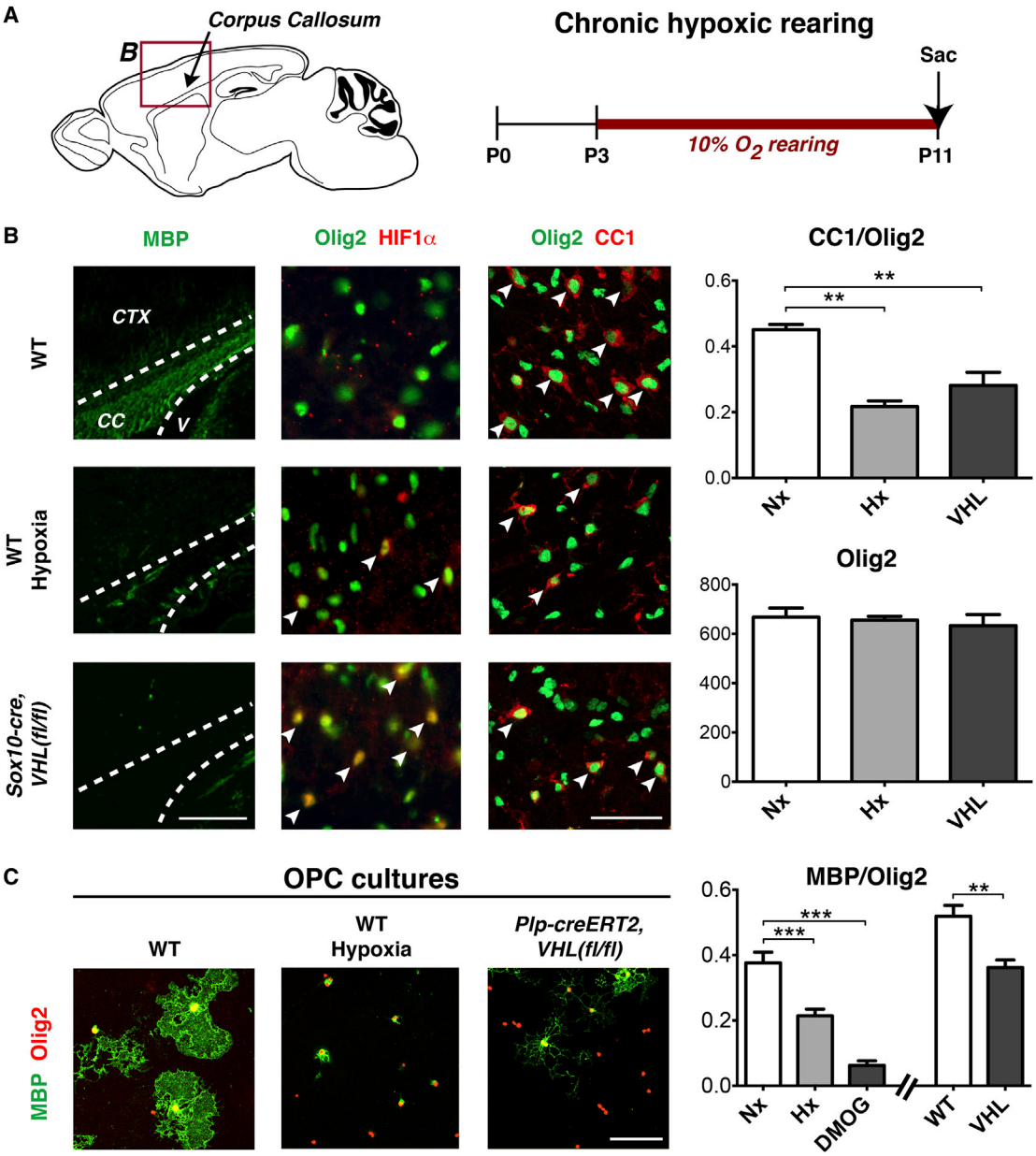

Figure 1. Oligodendrocyte-Specific *VHL* Deletion Inhibits Differentiation and Myelination

(A) Schematic of anatomical regions of corpus callosum (CC), cerebral cortex (CTX), and ventricle (V) presented in (B) and experimental timeline for chronic hypoxic rearing.

(B) Images showing hypomyelination, OL-lineage HIF1α expression, and OPC maturation arrest in CC of hypoxic WT mice or normoxic *Sox10-cre*, *VHL*(*fl/fl*) mice at P11. Arrowheads denote double-positive cells. Scale bar, 100 μm (MBP) and 50 μm (Olig2).

(C) Immunopurified OPCs exposed to hypoxia or isolated from *Plp-creERT2*, *VHL*(*fl/fl*) mice show differentiation block. Scale bar, 100 μm.

For quantifications, mean + SEM; n ≥ 3 experiments/genotype; **p < 0.01 and ***p < 0.001; one-way ANOVA with Dunnett's multiple comparison test. See also Figure S1.

of the activated form of β-catenin and the Wnt transcriptional targets Axin2, Notum, and Naked1 compared to controls. Similar findings were obtained in DMOG-treated immunopurified OPC cultures (Figure S3B), indicating that HIF stabilization activates canonical Wnt signaling in OPCs. As we used purified OPC cultures, these results also suggested that Wnt ligands produced by OPCs act in an autocrine fashion. To test this, we used IWP2, which inhibits Wnt ligand secretion by blocking porcupine function (Figure 3A; Chen et al., 2009). As shown (Figures 3C, 3D, and S3C), IWP2 was sufficient to reduce both hypomyelination and maturation arrest after hypoxia or OPC *VHL* loss of function. As a control for canonical Wnt pathway activity inhibition, we

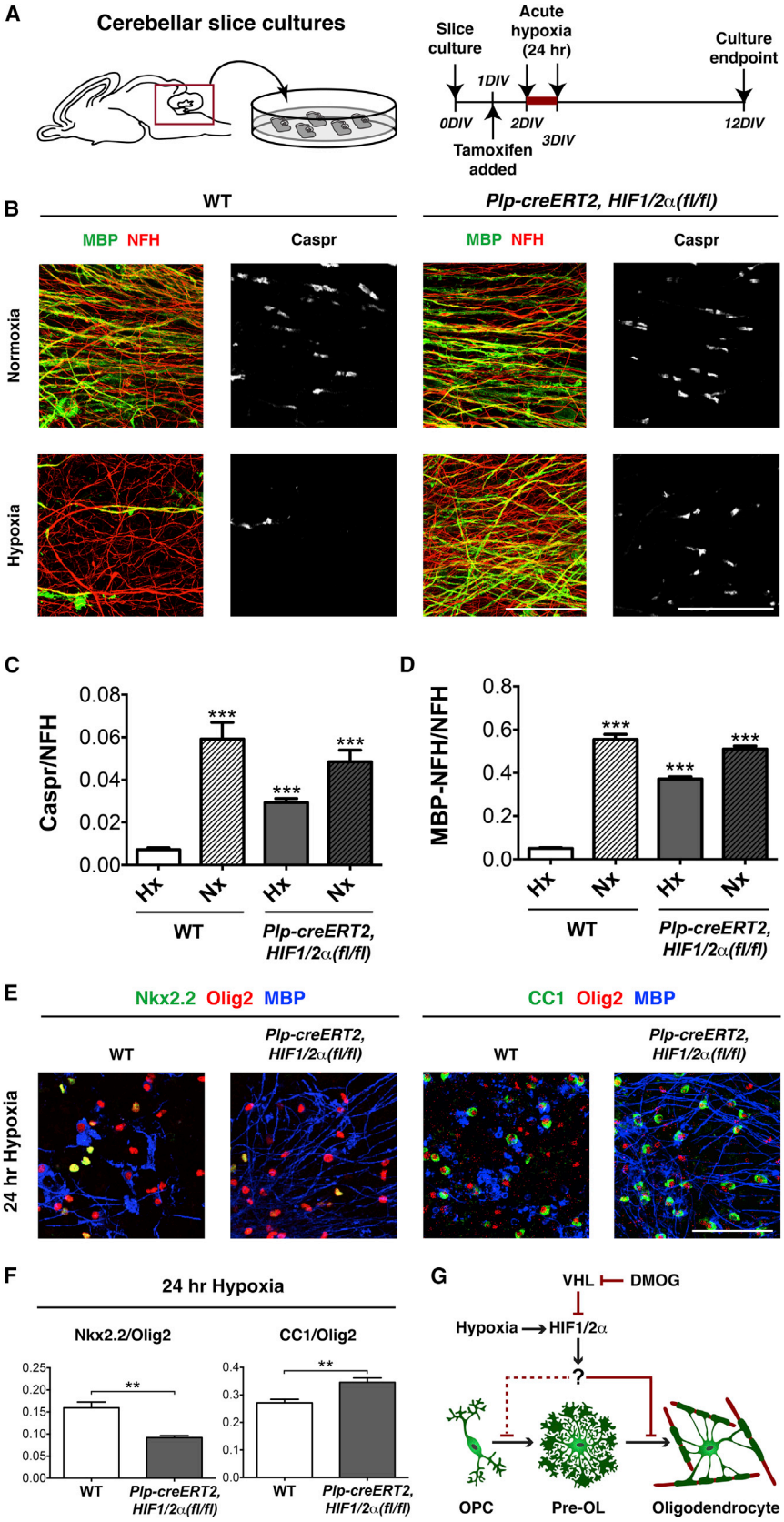

Figure 2. OPC-Encoded *HIF1/2α* Function Mediates Hypoxia-Induced Hypomyelination

(A) Schematic and timeline for cerebellar slice cultures (CSC) exposed to hypoxia.

(B) Removing *HIF1/2α* function in OLs significantly reduces hypoxia-induced hypomyelination in CSC. Scale bars, 25 μm (Caspr) and 50 μm (MBP/NFH). n ≥ 6 experiments/condition.

(C) Quantification of myelination in CSC.

(D) Additional quantification of myelination in CSC.

(E) Removing OPC *HIF1/2α* function significantly reduces hypoxia differentiation block in CSC. Scale bar, 100 μm.

(F) Quantification of OL differentiation showing Nkx2.2/Olig2 (OPCs) numbers decreased and CC1/Olig2 (mature OLs) numbers increased. Data were analyzed by t test, and significant differences (**p < 0.01) are shown.

(G) Model for HIF-induced OPC differentiation block.

Data in (C), (D) and (F) are mean + SEM; **p<0.01 and ***p<0.001; (C) and (D), one-way ANOVA with Dunnett's multiple comparison test; (F), t test. See also Figure S2.

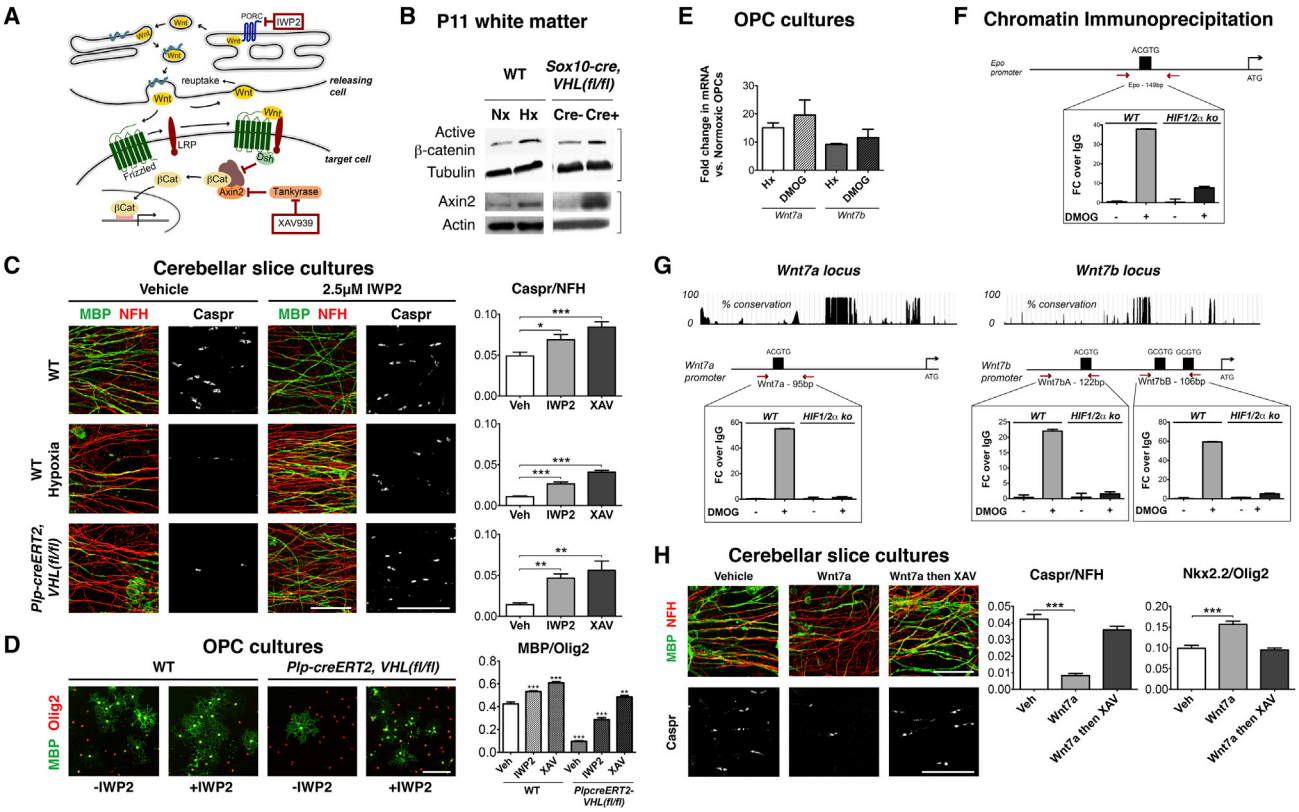

Figure 3. HIF Stabilization in OPCs Activates Canonical Wnt Signaling

(A) Schematic showing Wnt signaling and inhibition of ligand secretion and canonical activity by porcupine inhibitor IWP2 and XAV939, which stabilizes Axin2 to promote β-catenin degradation.

(B) Western blots of P11 white matter demonstrating upregulation of activated β-catenin and Axin2 levels in WT mice reared in hypoxia and normoxic *Sox10-cre*, *VHL*(*fl*/*fl*) mice (n = 3 animals/genotype).

(C) IWP2 prevents hypomyelination in CSC exposed to hypoxia or from *Plp-creERT2*, *VHL*(*fl*/*fl*) mice. Scale bars, 25 μm (Caspr) and 50 μm (MBP/NFH).

(D) OPC maturation arrest in *Plp-creERT2*, *VHL*(*fl*/*fl*) OPCs is attenuated by IWP2 or XAV939. Scale bar, 100 μm.

(E) Immunopurified OPCs cultured in hypoxic conditions or exposed to DMOG specifically upregulate *Wnt7a* and *Wnt7b* as shown by qRT-PCR (n = 3).

(F) Positive control for ChIP analysis at *Epo* locus.

(G) Mouse *HIF1/2α* KO and control embryonic fibroblasts cultured with/without DMOG (16 hr) assayed by ChIP. Following immunoprecipitation with antibodies against HIF1α or control (mouse IgG), DNA extracts were assessed by qRT-PCR. HIF1α bound to the *Wnt7a* locus at one HRE and *Wnt7b* locus via two HREs. Binding was not observed in DMOG-treated *HIF1/2α* mutant cells or non-DMOG-treated controls.

(H) Wnt7a proteins cause hypomyelination and OPC maturation arrest in CSC, which is reversed with XAV939. Scale bars, 25 μm (Caspr) and 50 μm (MBP/NFH).

Data shown are mean + SEM; n ≥ 3 experiments; *p<0.05, **p<0.01, and ***p<0.001; one-way ANOVA with Dunnett's multiple comparison test. See also Figure S3.

confirmed these effects with XAV939 (Figures 3A, 3C, 3D, and S3C–S3F). Thus, OPC HIF activation promotes the secretion of canonical Wnt ligand(s) that act in an autocrine manner to inhibit differentiation/myelination.

Evidence that *Wnt7a* and *Wnt7b* Are Direct HIF-Inducible Targets

Analysis of a database of genes expressed during OL development (Cahoy et al., 2008) revealed that *Wnt4*, *Wnt7a*, and *Wnt7b* are expressed at high levels in OPCs and become downregulated in mature OLs (Figure S3G). To further identify HIF targets, we performed qRT-PCR with primers for each of the 19 mammalian Wnt genes (Table S1) against mRNA from hypoxic or DMOG-treated OPCs. As shown (Figure 3E and Table S1), we observed upregulation of *Wnt7a* and *Wnt7b*, but not other Wnt genes.

To determine whether *Wnt7a* and/or *Wnt7b* are direct targets of HIF, we tested HRE (A/GTCTG) motifs proximal to the core promoters of these loci (see Extended Experimental Procedures) with chromatin immunoprecipitation (ChIP) in the presence/absence of DMOG to regulate HIF protein stability. Known HREs for *Epo* served as a positive control (Figure 3F), and HRE-negative upstream regions served as negative controls (Figure S3H). As shown (Figure 3G), anti-HIF1α antibody-mediated precipitation resulted in significant signal from putative *Wnt7a* or *Wnt7b* HREs and the *Epo* HRE in WT mouse embryonic fibroblasts (MEFs) treated with DMOG, but not *HIF1/2α* double-KO MEFs. These findings indicate that HIF1α proteins bind to

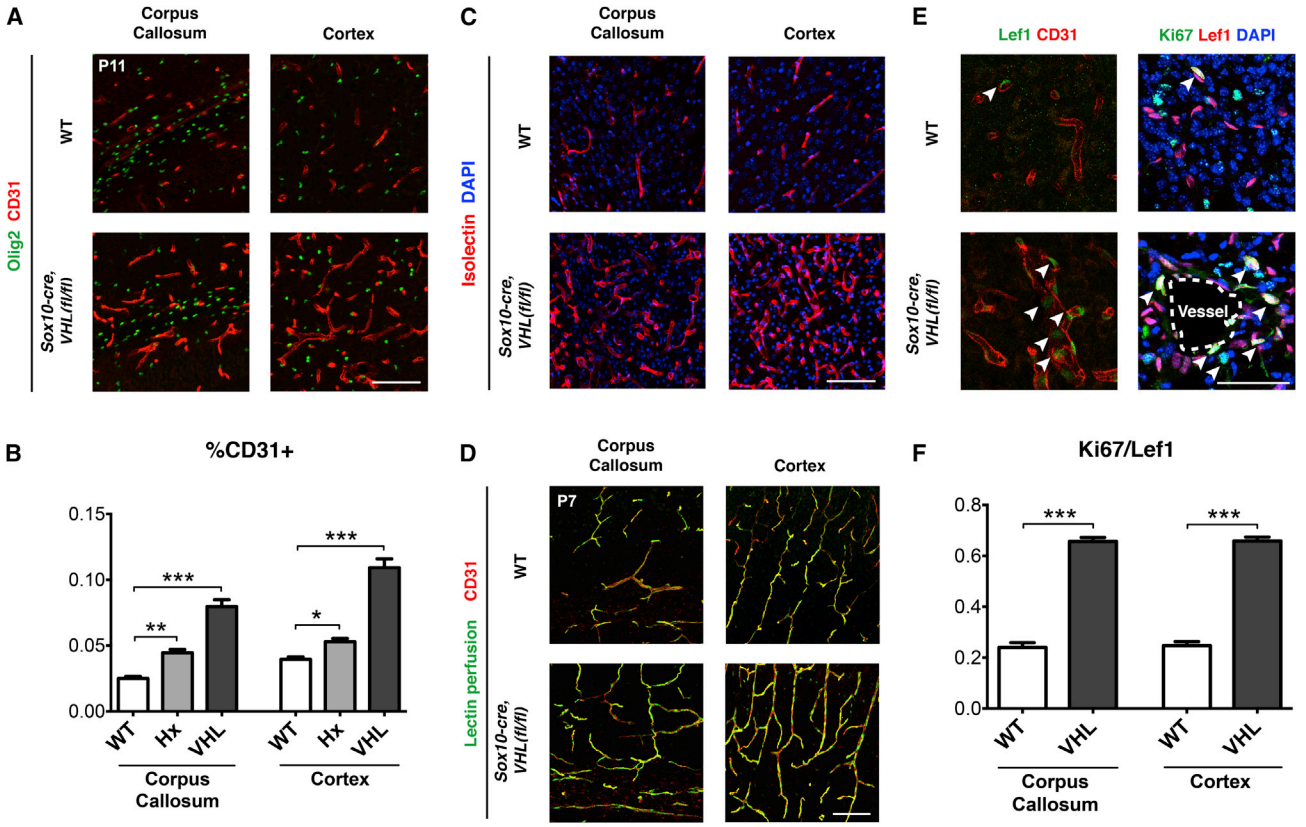

Figure 4. *HIF* Stabilization in OPCs Promotes Angiogenesis In Vivo

(A) Increased angiogenesis in *Sox10-cre*, *VHL*(*fl/fl*) mice as shown by expression of endothelial marker, CD31. Dense regions of Olig2 staining indicate white matter tracts in the corpus callosum. Scale bar, 100 μm. n ≥ 3 animals/genotype.

(B) Quantification of endothelial/vessel area (CD31+) demonstrates significant increases in hypoxic WT and normoxic *Sox10-cre*, *VHL*(*fl/fl*) mice. Data shown are mean + SEM and were analyzed by one-way ANOVA with Dunnett's multiple comparison test, and significant differences (*p < 0.05, **p < 0.05, and ***p < 0.001) are shown.

(C) Endothelial marker Isolectin demonstrating increased angiogenesis in *Sox10-cre*, *VHL*(*fl/fl*) mice. Scale bar, 100 μm.

(D) Isolectin perfusion in WT and *Sox10-cre*, *VHL*(*fl/fl*) mice indicating perfusion of blood vessels. Scale bar, 100 μm.

(E) Increased Lef1 expression in endothelia of *Sox10-cre*, *VHL*(*fl/fl*) mice. Of these, the majority are colabeled with the proliferation marker, Ki67. Scale bar, 50 μm. n ≥ 3 animals/genotype.

(F) Quantification of Ki67+/Lef1+ endothelial cells in corpus callosum and cortex. Data shown are mean + SEM and were analyzed by t test, and significant differences (***p < 0.001) are shown.

See also Figure S4 and Tables S1 and S3.

Wnt7a and *Wnt7b* HREs. Finally, we found that Wnt7a exposure resulted in OPC maturation arrest (increase in ratio of immature Nkx2.2/Olig2 cells) and hypomyelination that was rescued by XAV939 (Figure 3H, S3I, and S3J), which is consistent with roles as a HIF target downstream effector of canonical Wnt signaling in OPCs.

OPC HIF Signaling Promotes CNS Angiogenesis and Endothelial Cell Proliferation

Canonical Wnt signaling is essential for the formation of CNS vasculature in the embryo (Daneman et al., 2009; Stenman et al., 2008), and CNS angiogenesis persists postnatally through the sprouting and elongation of embryonically derived vessels during the first 10 days of murine life (Harb et al., 2013). Although angiogenic roles for OPCs are unprecedented, the findings above raised the possibility that *Wnt7a*/*7b* also had paracrine roles in white matter.

We first investigated whether OPC HIF stabilization affected postnatal vascular development in vivo. As shown (Figures 4A–4D and S4A), vascular density of *Sox10-cre*, *VHL*(*fl/fl*) mice was significantly increased, as indicated by endothelial markers CD31, isolectin, and Glut1. Similar findings were observed in *Olig1-cre*, *VHL*(*fl/fl*) mice (Figure S4B). Fate mapping for *Sox10-cre* and *Olig1-cre* drivers failed to show any contributions to endothelial or smooth muscle vascular cells (Table S3 and Figures S4C and S4D). We did observe that approximately 9% of white matter pericytes were fate mapped by *Sox10-cre* and *Olig1-cre* (Table S3 and Figure S4C), so we cannot rule out a small contribution of these cells. Despite increased vessel density, we found normal investment by pericytes and astrocyte

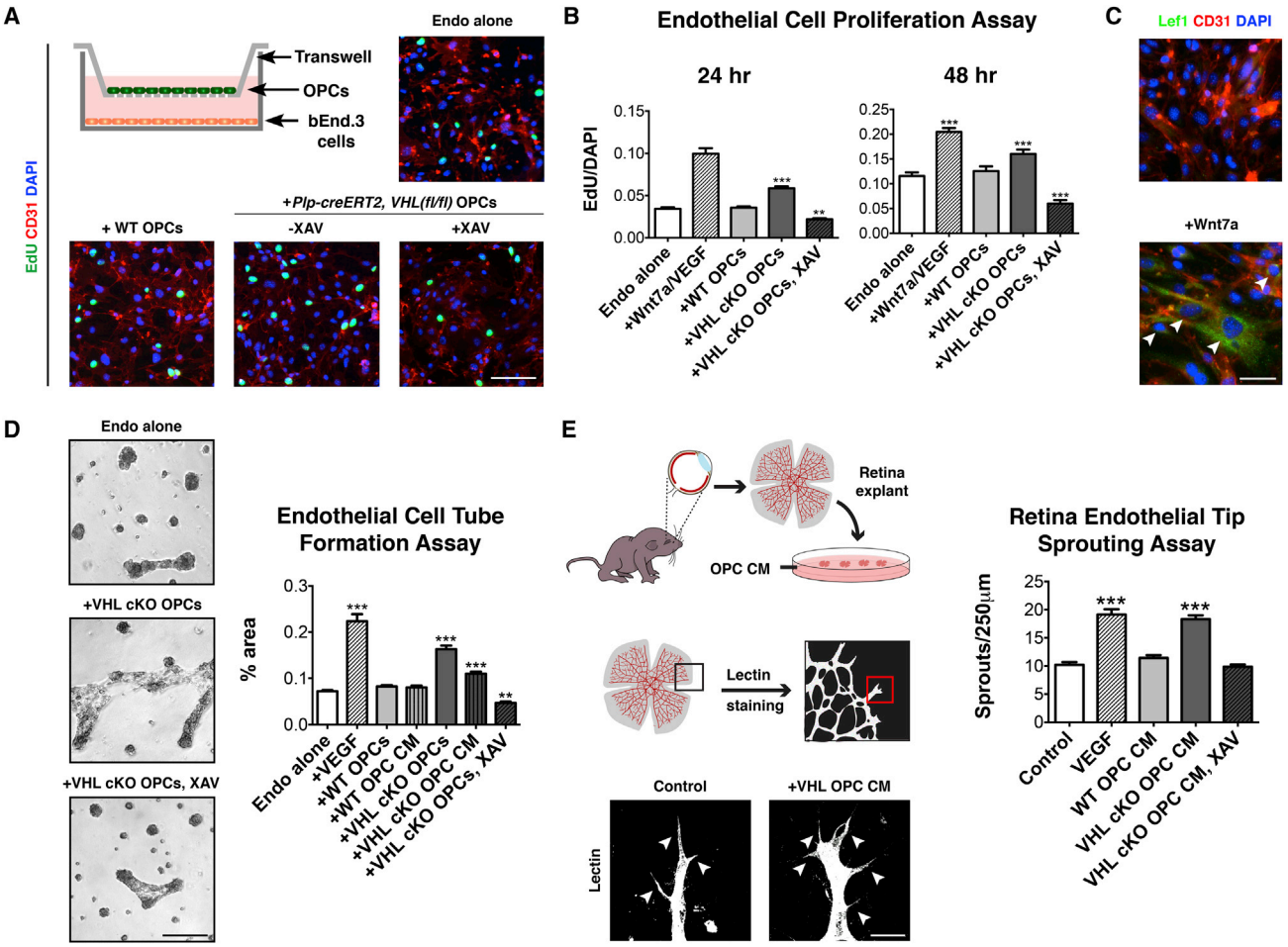

Figure 5. OPCs Directly Promote Angiogenesis in a Wnt-Dependent Manner

(A) Schematic showing transwell coculture assay for OPCs and bEnd.3 cells. OPCs from *Plp-creERT2*, *VHL*(*fl*/*fl*) mice induce endothelial cell proliferation in a Wnt-dependent manner. Scale bar, 100 μm.

(B) Quantification of endothelial cell proliferation in transwell assay at 24 hr and 48 hr.

(C) Wnt7a treatment of bEnd.3 cells induces Lef1 expression (arrowheads). Scale bar, 30 μm.

(D) Transwell cocultures of *Plp-creERT2*, *VHL*(*fl*/*fl*) OPCs and bEnd.3 cells promotes endothelial cell tube formation in a Wnt-dependent manner. Scale bar, 500 μm.

(E) Schematic showing retina endothelial tip sprouting assay. Conditioned medium from *Plp-creERT2*, *VHL*(*fl*/*fl*) OPCs promoted endothelial tip sprouting and filopodia extension in a Wnt-dependent manner. Scale bar, 25 μm.

For all quantifications, mean + SEM; n ≥ 3 experiments (A and B) and n ≥ 2 (D and E); $^{**}p < 0.01$ and $^{***}p < 0.001$; one-way ANOVA with Dunnett's multiple comparison test. See also Figure S5.

endfeet and no evidence for blood-brain barrier leakage as assessed by lectin perfusion, fibrinogen staining outside of the vasculature, and absence of hemorrhage (Figures 4D and S4E and data not shown).

We next analyzed activation of endothelial Wnt signaling by expression of the transcriptional target, Lef1 (Eastman and Grosschedl, 1999; Huber et al., 1996; Porfiri et al., 1997). As shown (Figure 4E), we found robust induction of Lef1 in CD31+ endothelial cells of *Sox10-cre*, *VHL*(*fl*/*fl*) mutants; moreover, the majority of these costained with the proliferation marker Ki67 (Figures 4E and 4F), suggesting that Wnt signaling promoted vessel growth. Although members of the vascular endothelial growth factor (VEGF) family are HIF target genes expressed within the OL lineage during development (Figure S4F) (Cahoy et al., 2008), we found no evidence for increased VEGF-A expression in OPCs of *Sox10-cre*, *VHL*(*fl*/*fl*) mice in vivo (Figure S4G). Thus, HIF stabilization in normoxic OPCs promotes angiogenesis, Wnt signaling, and endothelial proliferation in vivo.

OPCs Directly Promote Angiogenesis in a Wnt-Dependent Manner

The results above do not address whether angiogenic effects of OPCs were direct and/or contact mediated. As shown (Figures 5A–5C and S5A), addition of Wnt7a proteins to cultures of brain endothelial cell line bEnd.3 (ATCC) induced proliferation and Lef1 expression. To demonstrate direct effects of OPCs, we

performed a transwell assay with bEnd.3 cells (Figure 5A), which allows exchange of diffusible factors but prevents cell-cell contact. Addition of soluble Wnt7a and/or VEGF proteins resulted in proliferation of bEnd.3 cells (Figures 5A–5C and S5A). We also observed these effects with tamoxifen-induced *Plp-creERT2*, *VHL*(*fl/fl*) OPCs (Figures 5A–5C), which was inhibited by XAV939 (Figures 5A–5C, S5A, and S5B). In contrast, VEGF inhibitor SU5416 did not inhibit OPC-induced endothelial proliferation (Figure S5C).

We next assessed endothelial tube formation of bEnd.3 cells in matrigel. As shown (Figure 5D), tamoxifen-induced *Plp-creERT2*, *VHL*(*fl/fl*) OPCs (or treatment with conditioned medium) promoted endothelial tube formation in a Wnt-dependent manner. Finally, we investigated direct effects of OPCs to promote endothelial tip sprouting of blood vessels in explants of neonatal mouse retina (Sawamiphak et al., 2010). We found that conditioned medium from *VHL*-deficient OPCs promoted retinal endothelial tip sprouting and that such effects were inhibited by the addition of XAV939 (Figure 5E). Taken together, these results indicate that OPCs directly induce angiogenesis in a non-contact-dependent, Wnt-mediated manner.

Oligodendrocyte *HIF1/2α* Function Is Essential for Angiogenesis and Integrity of Corpus Callosum

To explore OPC *HIF* functions in vivo, we intercrossed *HIF1/2α*(*fl/fl*) mice with *Sox10-cre* and *Olig1-cre* lines. *Sox10-cre*, *HIF1/2α*(*fl/fl*) only survived until P4–P7. In contrast, *Olig1-cre*, *HIF1/2α*(*fl/fl*) mice were viable into adulthood as late as P90 (n = 5) but exhibited foot-clasping behavior (Figure S6A). The reasons for early lethality of *Sox10-cre*, *HIF1/2α*(*fl/fl*) mice compared to *Olig1-cre*, *HIF1/2α*(*fl/fl*) mice are unclear but likely reflect differential targeting patterns to precursor cells of the CNS and PNS.

As shown (Figure 6A), histological analysis demonstrated dramatic loss of forebrain white matter tracts and presence of cysts in the corpus callosum at P4–P7. To resolve distinct and/or overlapping contributions of *HIF1α* versus *HIF2α* in this white matter phenotype, we analyzed single, compound, and double-mutant animals. As shown (Figures 6A and 6C and Table S2), in P4 double-KO *Sox10-cre*, *HIF1/2α*(*fl/fl*) and *Olig1-cre*, *HIF1/2α*(*fl/fl*) mice, we observed macroscopic and microscopic acellular cysts in the corpus callosum typically located at the boundary with adjacent gray matter structures (neocortex, striatum). In contrast, single *HIF1α* or *HIF2α* mutants showed minimal effects, and compound mutants that were *HIF1α*(*fl/fl*);*HIF2α*(*fl/+*) or *HIF1α*(*fl/+*);*HIF2α*(*fl/fl*) showed only corpus callosum microcysts. Thus, OPC intrinsic *HIF1α* and *HIF2α* show partially overlapping yet essential functions in white matter development.

In order to determine the basis for white matter loss, we assessed the ontogeny of OLs and the brain vasculature at E18, P4, and P7. Although the brain of E18 *Olig1-cre*, *HIF1/2α*(*fl/fl*) mice had a grossly normal appearance and density of CD31+ endothelia (Figures 6A and 6B), dysgenesis of the forebrain white matter suggested abnormalities in OPC-induced angiogenesis with onset between P0 and P7. Indeed, we observed that the density of CD31+ endothelia in corpus callosum showed a significant decrease at P4 in *Olig1-cre*, *HIF1/2α*(*fl/fl*) mice (Figure 6B). The P4 time point also showed high levels of cleaved Caspase3 (Casp3)+ apoptotic cells in the mutant white matter (Figure 6C), including activated CD68+ microglia/macrophages, Olig2+ OLs, PDGFRα+ OPCs, and GFAP+ astrocytes (Figure S6B). Despite this, numbers of Olig2+ cells in the white matter of *Olig1-cre*, *HIF1/2α*(*fl/fl*) mice were only about 15% diminished at P4 compared to WT, whereas we observed a 40% reduction at E18 (Figure 6B). Strikingly, the P4 mutant corpus callosum showed evidence of severe axonal damage as assessed by SMI32 and Casp3 expression (Figures 6D and 6E). Together, these findings indicate a sequence of deficient angiogenesis at P4, which leads to a general deterioration of white matter, resulting in acellular cysts by P7 (Figure 6A). Thus, combined *HIF1/2α* function in OPCs is necessary to promote postnatal white matter angiogenesis and maintain structural integrity of the corpus callosum.

HIF Loss of Function in OPCs Is Permissive for Cortical Vessel and Projection Neuron Development

We next investigated the impact of OPC *HIF* deletion on cortical plate development. The mammalian neocortex is divided into six layers (Dugas-Ford et al., 2012). As shown in Figure 7A, although the cortical plate is thinner in *Olig1-cre*, *HIF1/2α*(*fl/fl*) mice at P7, its component layers are intact. In contrast to findings in white matter (Figure 6B), vessel density in the P4 cortex of *Olig1-cre*, *HIF1/2α*(*fl/fl*) mice was not significantly different than controls (Figure 7B). In addition, layer 2/3 neurons, marked by expression of SATB2 (Alcamo et al., 2008), as well as layer 5/6 neuron populations, appeared to be preserved (Figure 7C).

We next used the HIF target BNIP3 (Bruick, 2000; Lee and Paik, 2006) as a physiologic readout of HIF pathway activity in WT and *Olig1-cre*, *HIF1/2α*(*fl/fl*) mutant animals. As shown (Figure 7D), BNIP3 is normally expressed at low levels in a subset of Olig2+ cells in the white matter of WT P4 mice. This indicates that a state of "physiological" hypoxia/HIF activation in normal white matter development, whereas cells in the cortex are mostly BNIP3 negative (Figure 7E). In contrast, we observed elevated numbers of BNIP3+ cells in the white matter and layers 5/6 of *Olig1-cre*, *HIF1/2α*(*fl/fl*) mice, indicating an abnormal state of hypoxia in these structures (Figures 7D and 7E); layer 2/3 neurons did not show increased BNIP3. As expected, we did not observe Olig2+/BNIP3+ cells in *Olig1-cre*, *HIF1/2α*(*fl/fl*) mice (Figure 7D). In summary, these findings suggest that deterioration of forebrain white matter tracts in *Olig1-cre*, *HIF1/2α*(*fl/fl*) is a primary—rather than a consequent—effect of deficient OPC-encoded HIF signaling on cortical plate projection neurons.

DISCUSSION

Developing appropriate white matter blood flow is essential given the high metabolic demands of myelinating OLs and the axons they invest. Though classic papers have noted the anatomical relationship of OLs to blood vessels (Cammermeyer, 1960; Del Rio-Hortega, 2012), our results demonstrate that OLs are critical regulators of postnatal CNS angiogenesis. We find that OPC-encoded HIF signaling coordinates the onset of postnatal myelination with establishment of adequate vasculature in the white matter through autocrine and paracrine Wnt activities, respectively (Figure S7).

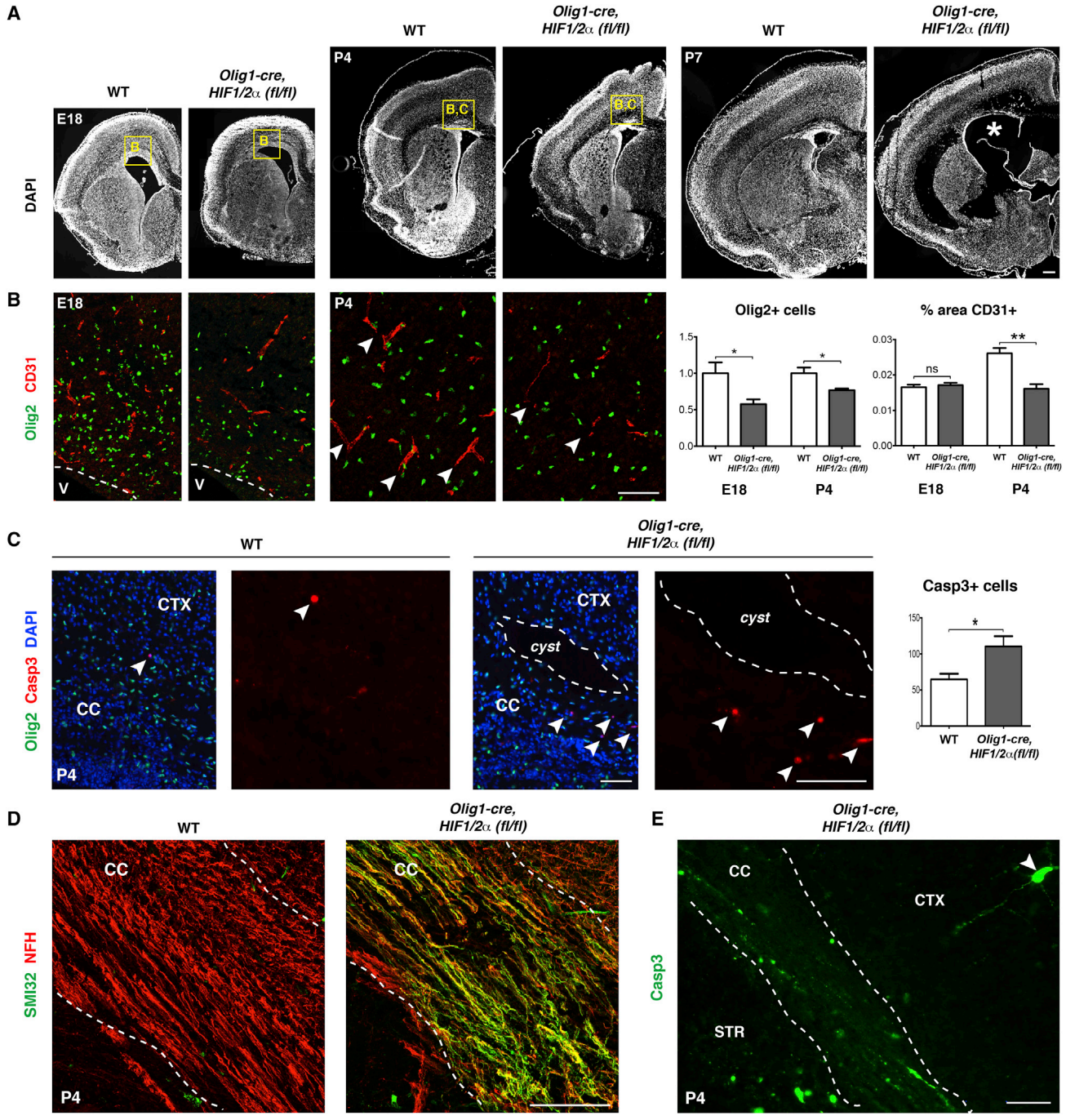

Figure 6. Oligodendrocyte *HIF1/2α* Function Is Required for Postnatal Angiogenesis and Maintenance of White Matter Integrity

(A) DAPI-stained sections at E18, P4, and P7 of mutant and control brains show white matter cysts (white asterisk) and dysgenesis by P7 in *Olig1-cre*, *HIF1/2α(fl/fl)* mice. n ≥ 3 animals/genotype. Scale bar, 100 μm.

(B) Olig2+ cells are reduced by ~40%, compared to WT at E18 and ~15% at P4. Vessel density in SVZ at E18 is similar in WT and mutant mice, whereas *Olig1-cre*, *HIF1/2α(fl/fl)* mice show significantly decreased vessel density at P4 in corpus callosum. Data shown are mean + SEM and were analyzed by t test, and significant differences (*$p < 0.05$ and **$p < 0.01$) are shown. Scale bar, 100 μm.

(C) White matter cysts and increased apoptotic cells (Casp3+) in P4 in *Olig1-cre*, *HIF1/2α(fl/fl)* mice. Data shown are mean + SEM and were analyzed by t test, and the significant difference (*$p < 0.05$) is shown. Scale bar, 100 μm (merged) and 50 μm (Casp3).

(D) Widespread axonal damage, indicated by SMI32+ staining, observed at P4 throughout the corpus callosum of *Olig1-cre*, *HIF1/2α(fl/fl)* mice. Scale bar, 100 μm.

(E) Robust Casp3 staining in axons of P4 *Olig1-cre*, *HIF1/2α(fl/fl)* corpus callosum. Note relative paucity of staining in cortex. Scale bar, 100 μm. See also Figure S6 and Tables S2 and S3.

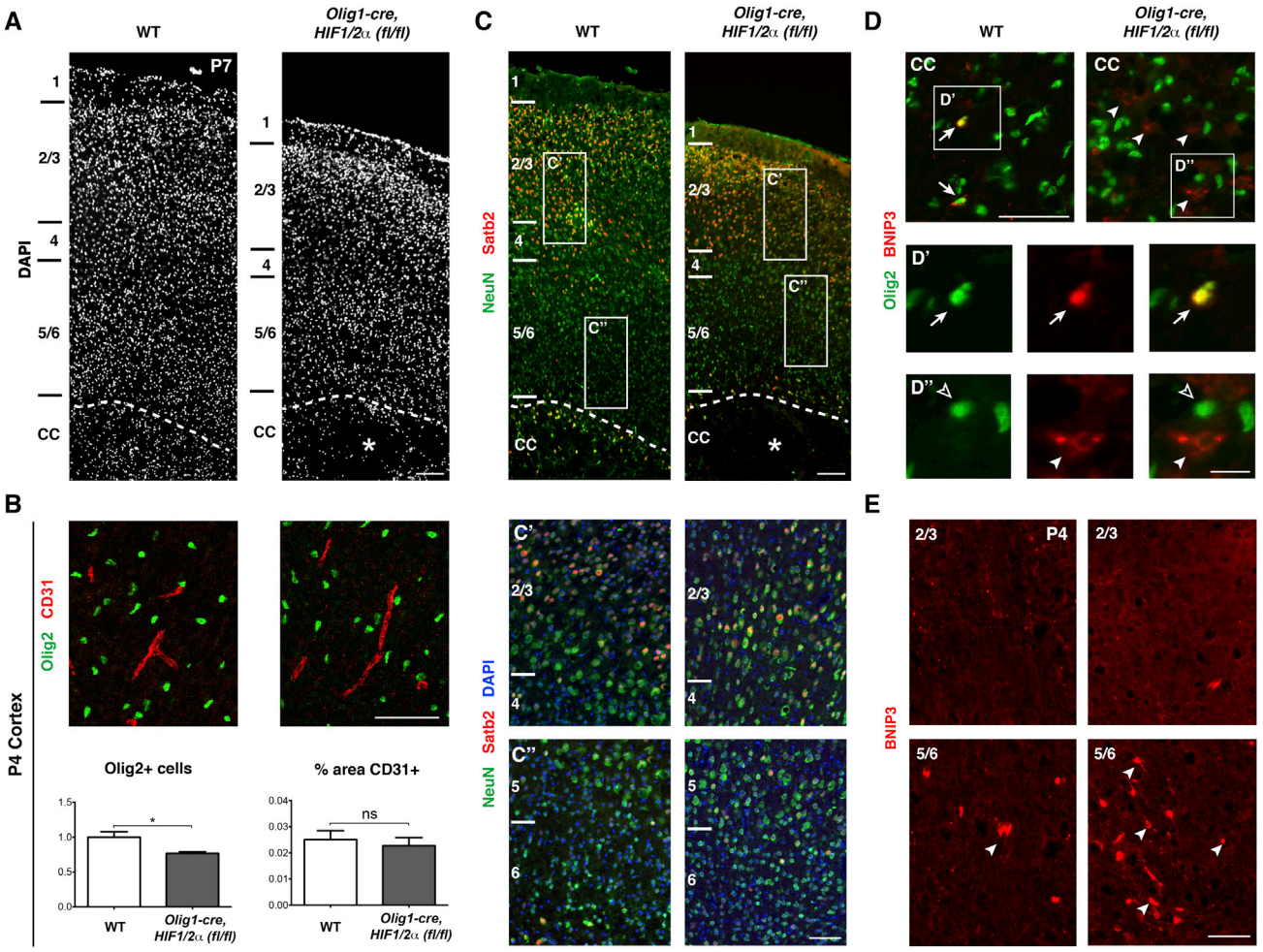

Figure 7. Loss of OPC *HIF1/2α* Function Is Permissive for Cortical Development and Angiogenesis

(A) DAPI stain of primary motor cortex in WT versus *Olig1-cre*, *HIF1/2α(fl/fl)* mice at P7 showing a thinner cortex in *Olig1-cre*, *HIF1/2α(fl/fl)* with the cortical layers and overall structure intact. Cortical layers are labeled to the left, and the asterisk denotes white matter cyst. n = 3 animals/genotype. Scale bar, 200 μm.

(B) OL numbers are reduced by ~23% in *Olig1-cre*, *HIF1/2α(fl/fl)* cortex, but vessel density (%CD31) is not statistically different. Data shown are mean + SEM and were analyzed by a two-tailed Student's t test, and the significant difference (*$p < 0.05$) is shown. n = 3 animals/genotype. Scale bar, 100 μm.

(C) Images of NeuN (green, pan-neuron marker), SatB2 (red, layer 2/3 callosal projection neurons), and DAPI providing further evidence that the cortex is grossly intact with ample numbers of callosal projection neurons. Note in higher magnification panels (C′ and C″) that cell density is grossly normal in *Olig1-cre*, *HIF1/2α(fl/fl)* cortex. Scale bars, 200 μm and 100 μm (insets).

(D) Images of the corpus callosum stained for BNIP3 (red) and Olig2 (green). In WT, BNIP3 is expressed in a subset of Olig2+ cells (arrows, D′ insets). In *Olig1-cre*, *HIF1/2α(fl/fl)* mice, whereas BNIP3 is not expressed in Olig2+ cells, aberrant expression of BNIP3 in non-Olig2+ cells (arrowheads, D″ insets) is indicative of the general hypoxic microenvironment. Scale bars, 100 μm and 20 μm (insets).

(E) Images of BNIP3 staining in dorsal cortex (top row) and ventral cortex (bottom row). BNIP3 is enriched in ventral cortex, but not in dorsal cortex, suggesting selective hypoxia in gray matter regions adjacent to the corpus callosum, but not more dorsal areas. n = 3 animals/genotype. Scale bar, 100 μm.

See also Figure S7 and Table S7.

Oxygen Tension Is a Developmental Regulator of Postnatal Myelination

Activity-dependent neuronal signals are thought to induce myelination (Demerens et al., 1996; Ishibashi et al., 2006; Stevens et al., 2002), and such coordination is important, in part, because myelin constrains axon outgrowth and synaptogenesis (Chong et al., 2012; Hu and Strittmatter, 2004). Our results suggest another level of regulation to ensure the presence of adequate blood supply and oxygen levels as a prerequisite for myelination to commence under appropriate physiological conditions. We propose an integrated HIF-regulated developmental mechanism (Figure S7) wherein OPCs that initially invest hypovascularized white matter are exposed to hypoxia, activate HIF signaling, and produce Wnt ligands, which, in turn, trigger angiogenesis. With increased oxygen delivery, HIF signaling becomes downregulated, thus allowing for OPC maturation and myelination to take place. This dual mechanism helps to ensure that myelination will only proceed when blood supply is sufficient to meet attendant metabolic demands. In culture, we could uncouple this relationship (by providing substrates and oxygen) and

confirm that *HIF* loss of function rescued hypoxia-induced hypomyelination. Thus, *HIF* function is necessary and sufficient for effects of oxygen levels on OPC maturation. Future studies are needed to determine whether HIF signaling also regulates OL development antenatally in the hypoxic intrauterine environment. We did observe that OPC numbers were deficient in *Olig1-cre*, *HIF1/2α*(*fl/fl*) animals at E18, which is consistent with this possibility.

Autocrine Wnt Signaling Functions Downstream of Hypoxia/HIF in OPCs

Canonical Wnt signaling inhibits OPC maturation during development and in disease (Fancy et al., 2009, 2011b; Ye et al., 2009a), and our studies show that HIF stabilization activates cell-autonomous Wnt production. HIF1α directly binds conserved HREs at the *Wnt7a* and *Wnt7b* loci, and stabilization of HIF in OPCs resulted in upregulation of *Wnt7a*/*7b*. Further studies are required to establish *Wnt7a*/*7b* as the specific downstream effectors of HIF signaling in OPCs, as other candidates (e.g., *Wnt4* and *Wnt5a*) are expressed in the OL lineage (Cahoy et al., 2008; Fancy et al., 2009). Although HIF stabilization in OPCs prevented postnatal maturation, we did not observe precocious myelination (e.g., with prenatal onset) in *Olig1-cre*, *HIF1/2α*(*fl/fl*) animals. This might suggest that downregulation of HIF signaling must also integrate with positive cues (e.g., axonal activity-dependent signals) for myelination to commence. Alternatively, it is possible that loss of *HIF* function results in the rapid death and removal of precociously maturing OLs.

OPCs Regulate White Matter Angiogenesis through Paracrine Wnt Signaling

Postnatal forebrain angiogenesis is characterized by sprouting/ingrowth of blood vessels toward white matter regions from P0 to P14 in mice (Harb et al., 2013; Sapieha, 2012). Conditional KO of *HIF1/2α* in OPCs resulted in deficient angiogenesis at P4 and ensuing deterioration of large white matter tracts, such as corpus callosum by P7. Conversely, OPC HIF stabilization resulted in increased expression of the proangiogenic genes *Wnt7a*/*7b* and overproduction of blood vessels characterized by robust populations of Lef1+ endothelia. Although VEGF is expressed by neurons, astrocytes, and microglia in response to hypoxia (Rosenstein et al., 2010), we did not observe VEGF induction by OPC-specific HIF stabilization. Our findings suggest dual functions for HIF-mediated Wnt signaling that couple OPC maturation and white matter vascular development. Although *Wnt7a*/*7b* are required for angiogenesis, their functions are dispensable after mature blood vessel structure is achieved (Daneman et al., 2009; Stenman et al., 2008); moreover, depletion of OLs in the adult brain (e.g., cuprizone-induced demyelination model) does not result in vascular abnormalities. These findings indicate roles of OPCs and Wnt signaling in angiogenesis, but not in the maintenance of mature vascular structure.

Oligodendrocyte HIF Signaling Is Essential for Developing White Matter Integrity

Mature OLs provide metabolic support for axons by supplying ATP, glycolytic substrates, and nutrients (Fünfschilling et al., 2012; Harris and Attwell, 2012; Lee et al., 2012; Rinholm et al., 2011). Here, we demonstrate that loss of *HIF* function in OPCs results in cell death, axon damage, and the appearance of cysts in white matter at P4 followed by a catastrophic loss of axons at P7 in the corpus callosum. Preliminary analysis indicates that this is also the case in white matter tracts throughout the forebrain, including internal capsule and striatum, whereas white matter tracts of the cerebellum and brainstem are preserved. These differences might reflect region-restricted roles for OPCs in white matter angiogenesis or, alternatively, regional variations in metabolic requirements of OPCs and/or the axons they invest. Although our findings indicate that white matter deterioration from P4 to P7 results from inadequate vascular investment, HIF signaling within OLs might also produce trophic factors for axons. Although such cysts may result from a failure of myelination, we think this is unlikely because the phenotype is observed in P7 corpus callosum before axons are normally myelinated.

Potential Roles for Oligodendrocytes in CNS Injury

OLs are early responders to a broad spectrum of brain pathologies, including demyelinating disorders (e.g., multiple sclerosis, MS), stroke, and penetrating trauma (Chang et al., 2002; Hampton et al., 2004; Kuhlmann et al., 2008; Tanaka et al., 2001). The notion that OPCs might produce angiogenic factors to encourage revascularization of injured CNS tissue is consistent with recent studies (Cayre et al., 2013; Jiang et al., 2011; Pham et al., 2012). Our finding of cystic changes in the white matter of OPC HIF null mice is reminiscent of periventricular leukomalacia, a condition observed in the brain of preterm infants. White matter injury induced by experimental autoimmune encephalomyelitis results in local tissue hypoxia (Davies et al., 2013), and OL HIF1α expression has been reported in MS lesions (Aboul-Enein et al., 2003). Further studies are needed to determine roles for OPCs as mediators of vascular remodeling after white matter injury. In summary, our findings demonstrate that cell-intrinsic HIF pathway function in OPCs couples postnatal myelination and angiogenesis during a critical window of early postnatal development.

EXPERIMENTAL PROCEDURES

Animals

All experimental procedures were approved by the Institutional Animal Care and Use Committee and Laboratory Animal Resource Center at UCSF. Mouse colonies were maintained in accordance with NIH and UCSF guidelines. *Sox10-cre* (Stolt et al., 2006), *Olig1-cre* (Lu et al., 2002), *Plp-CreERT2* (Doerflinger et al., 2003), *VHL floxed* (Rankin et al., 2005), *HIF1α floxed* (Ryan et al., 2000), and *HIF2α floxed* (Gruber et al., 2007) mice have been previously described.

Cerebellar Slice Cultures

Mouse explant cerebellar slice cultures were generated from P0–P1 mouse pups and cultured for 12 days in vitro (DIV). Tamoxifen (Sigma) was added to transgenic cultures at 1 DIV and 3 DIV. Hypoxic and DMOG cultures were exposed to hypoxia (2% FiO_2) or DMOG (Sigma) between 2 and 3 DIV. Factors were added after hypoxia or DMOG treatment and were replenished every other day. See Extended Experimental Procedures for more details.

qRT-PCR

RNA was isolated (Trizol extraction followed by RNeasy; QIAGEN) from immunopurified OPC cultures and assayed for gene expression by SYBR-Green on a Lightcycler 480 (Roche).

Western Blots

Protein was extracted using standard protocols (Kenney et al., 2003) and then detected by either an Amersham ECL luminescence kit (GE Healthcare) or by immunofluorescence using the Li-Cor detection system (Li-Cor).

Chromatin Immunoprecipitation DNA-Binding Assays

Chromatin IP for HIF1α was conducted using the Human/Mouse HIF-1α ExactaChIP Chromatin IP kit (R&D Systems) followed by qRT-PCR with primers flanking HREs in genomically conserved domains proximal to *Wnt7a* and *Wnt7b* core promoter regions. See Extended Experimental Procedures for more details.

OPC-Endothelial Cell Transwell Assays

Mouse immunopurified OPCs were plated on transwell inserts (Corning), and mouse brain endothelial cells (bEnd.3 cell line, ATCC CRL-2299) were plated on PDL-coated glass coverslips below. Proliferation was assessed with EdU labeling at 24 hr and 48 hr.

Endothelial Tube Formation Assay

bEnd.3 cells were plated on a matrigel matrix (BD), and factors or transwell inserts with OPCs were added. Following incubation for 18 hr, endothelial cell tube formation was imaged under phase contrast.

Retinal Explants

Retinas from P4–P5 CD1 mice were dissected and flat mounted on Millicell inserts and allowed to recover for 2 to 4 hr, after which factors or OPC conditioned medium were added. After 4 to 6 hr, explants were fixed and stained with Isolectin GS-IB4.

Statistical Analyses

For all quantified data, mean + SEM values are presented. Statistical significance was determined using unpaired, two-tailed Student's t tests, as well as one-way ANOVA with Dunnett's multiple comparison test (GraphPad Prism).

SUPPLEMENTAL INFORMATION

Supplemental Information includes Extended Experimental Procedures, seven figures, and three tables and can be found with this article online at http://dx.doi.org/10.1016/j.cell.2014.04.052.

AUTHOR CONTRIBUTIONS

T.J.Y. and J.C.S. performed all experiments and data analysis except the following: A.G. and S.M.C. assisted with immunostaining and genotyping; R.D., S.P.J.F., and E.M. provided advice on experimental design and reagents; H.Z. designed and optimized primers; and T.J.Y., J.C.S., and D.H.R. designed all experiments and wrote the manuscript.

ACKNOWLEDGMENTS

We are grateful to Emily Harrington and April Tenney for expert technical help and Matt Rasband, Nenad Sestan, and Klaus Nave for discussions. We thank Andrew McMahon (USC) for genomic sequence information for *Wnt7a* and *7b* loci, William Kaelin (Dana-Farber Cancer Institute) for floxed *VHL* transgenic mice, and William Richardson (UCL) for *Sox10-cre* transgenic mice. We also thank Nina Bauer, who drew all illustrations. T.J.Y. acknowledges a postdoctoral fellowship from the National Multiple Sclerosis Society (NMSS). J.C.S. acknowledges support from training grant T32 GM007449-36 from NIGMS and the Ruth Kirschstein NRSA fellowship F31 NS076254-03 from NINDS. This work was made possible by grants from NICHD (HD072544 to E.M.), NMSS (to D.H.R.) and NINDS (NS040511 and P01NS083513 to D.H.R.). D.H.R. is a HHMI Investigator.

Received: December 8, 2013
Revised: March 13, 2014
Accepted: April 22, 2014
Published: July 10, 2014

REFERENCES

Aboul-Enein, F., Rauschka, H., Kornek, B., Stadelmann, C., Stefferl, A., Brück, W., Lucchinetti, C., Schmidbauer, M., Jellinger, K., and Lassmann, H. (2003). Preferential loss of myelin-associated glycoprotein reflects hypoxia-like white matter damage in stroke and inflammatory brain diseases. J. Neuropathol. Exp. Neurol. *62*, 25–33.

Alcamo, E.A., Chirivella, L., Dautzenberg, M., Dobreva, G., Fariñas, I., Grosschedl, R., and McConnell, S.K. (2008). Satb2 regulates callosal projection neuron identity in the developing cerebral cortex. Neuron *57*, 364–377.

Baron, W., and Hoekstra, D. (2010). On the biogenesis of myelin membranes: sorting, trafficking and cell polarity. FEBS Lett. *584*, 1760–1770.

Bradl, M., and Lassmann, H. (2010). Oligodendrocytes: biology and pathology. Acta Neuropathol. *119*, 37–53.

Bruick, R.K. (2000). Expression of the gene encoding the proapoptotic Nip3 protein is induced by hypoxia. Proc. Natl. Acad. Sci. USA *97*, 9082–9087.

Cahoy, J.D., Emery, B., Kaushal, A., Foo, L.C., Zamanian, J.L., Christopherson, K.S., Xing, Y., Lubischer, J.L., Krieg, P.A., Krupenko, S.A., et al. (2008). A transcriptome database for astrocytes, neurons, and oligodendrocytes: a new resource for understanding brain development and function. J. Neurosci. *28*, 264–278.

Cammermeyer, J. (1960). Reappraisal of the perivascular distribution of oligodendrocytes. Am. J. Anat. *106*, 197–231.

Cayre, M., Courtès, S., Martineau, F., Giordano, M., Arnaud, K., Zamaron, A., and Durbec, P. (2013). Netrin 1 contributes to vascular remodeling in the subventricular zone and promotes progenitor emigration after demyelination. Development *140*, 3107–3117.

Chang, A., Tourtellotte, W.W., Rudick, R., and Trapp, B.D. (2002). Premyelinating oligodendrocytes in chronic lesions of multiple sclerosis. N. Engl. J. Med. *346*, 165–173.

Chen, B., Dodge, M.E., Tang, W., Lu, J., Ma, Z., Fan, C.W., Wei, S., Hao, W., Kilgore, J., Williams, N.S., et al. (2009). Small molecule-mediated disruption of Wnt-dependent signaling in tissue regeneration and cancer. Nat. Chem. Biol. *5*, 100–107.

Chong, S.Y., Rosenberg, S.S., Fancy, S.P., Zhao, C., Shen, Y.A., Hahn, A.T., McGee, A.W., Xu, X., Zheng, B., Zhang, L.I., et al. (2012). Neurite outgrowth inhibitor Nogo-A establishes spatial segregation and extent of oligodendrocyte myelination. Proc. Natl. Acad. Sci. USA *109*, 1299–1304.

Chrast, R., Saher, G., Nave, K.A., and Verheijen, M.H. (2011). Lipid metabolism in myelinating glial cells: lessons from human inherited disorders and mouse models. J. Lipid Res. *52*, 419–434.

Daneman, R., Agalliu, D., Zhou, L., Kuhnert, F., Kuo, C.J., and Barres, B.A. (2009). Wnt/beta-catenin signaling is required for CNS, but not non-CNS, angiogenesis. Proc. Natl. Acad. Sci. USA *106*, 641–646.

Daneman, R., Zhou, L., Kebede, A.A., and Barres, B.A. (2010). Pericytes are required for blood-brain barrier integrity during embryogenesis. Nature *468*, 562–566.

Davies, A.L., Desai, R.A., Bloomfield, P.S., McIntosh, P.R., Chapple, K.J., Linington, C., Fairless, R., Diem, R., Kasti, M., Murphy, M.P., and Smith, K.J. (2013). Neurological deficits caused by tissue hypoxia in neuroinflammatory disease. Ann. Neurol. *74*, 815–825.

Del Rio-Hortega, P. (2012). Are the glia with very few processes homologous with Schwann cells? by Pío del Río-Hortega. 1922. Clin. Neuropathol. *31*, 460–462.

Demerens, C., Stankoff, B., Logak, M., Anglade, P., Allinquant, B., Couraud, F., Zalc, B., and Lubetzki, C. (1996). Induction of myelination in the central nervous system by electrical activity. Proc. Natl. Acad. Sci. USA *93*, 9887–9892.

Doerflinger, N.H., Macklin, W.B., and Popko, B. (2003). Inducible site-specific recombination in myelinating cells. Genesis *35*, 63–72.

Dugas-Ford, J., Rowell, J.J., and Ragsdale, C.W. (2012). Cell-type homologies and the origins of the neocortex. Proc. Natl. Acad. Sci. USA *109*, 16974–16979.

Eastman, Q., and Grosschedl, R. (1999). Regulation of LEF-1/TCF transcription factors by Wnt and other signals. Curr. Opin. Cell Biol. *11*, 233–240.

Emery, B., and Dugas, J.C. (2013). Purification of oligodendrocyte lineage cells from mouse cortices by immunopanning. Cold Spring Harb. Protoc. *2013*, 854–868.

Fancy, S.P., Baranzini, S.E., Zhao, C., Yuk, D.I., Irvine, K.A., Kaing, S., Sanai, N., Franklin, R.J., and Rowitch, D.H. (2009). Dysregulation of the Wnt pathway inhibits timely myelination and remyelination in the mammalian CNS. Genes Dev. *23*, 1571–1585.

Fancy, S.P., Chan, J.R., Baranzini, S.E., Franklin, R.J., and Rowitch, D.H. (2011a). Myelin regeneration: a recapitulation of development? Annu. Rev. Neurosci. *34*, 21–43.

Fancy, S.P., Harrington, E.P., Yuen, T.J., Silbereis, J.C., Zhao, C., Baranzini, S.E., Bruce, C.C., Otero, J.J., Huang, E.J., Nusse, R., et al. (2011b). Axin2 as regulatory and therapeutic target in newborn brain injury and remyelination. Nat. Neurosci. *14*, 1009–1016.

Franceschini, M.A., Thaker, S., Themelis, G., Krishnamoorthy, K.K., Bortfeld, H., Diamond, S.G., Boas, D.A., Arvin, K., and Grant, P.E. (2007). Assessment of infant brain development with frequency-domain near-infrared spectroscopy. Pediatr. Res. *61*, 546–551.

Fünfschilling, U., Supplie, L.M., Mahad, D., Boretius, S., Saab, A.S., Edgar, J., Brinkmann, B.G., Kassmann, C.M., Tzvetanova, I.D., Möbius, W., et al. (2012). Glycolytic oligodendrocytes maintain myelin and long-term axonal integrity. Nature *485*, 517–521.

Gruber, M., Hu, C.J., Johnson, R.S., Brown, E.J., Keith, B., and Simon, M.C. (2007). Acute postnatal ablation of Hif-2alpha results in anemia. Proc. Natl. Acad. Sci. USA *104*, 2301–2306.

Hampton, D.W., Rhodes, K.E., Zhao, C., Franklin, R.J., and Fawcett, J.W. (2004). The responses of oligodendrocyte precursor cells, astrocytes and microglia to a cortical stab injury, in the brain. Neuroscience *127*, 813–820.

Harb, R., Whiteus, C., Freitas, C., and Grutzendler, J. (2013). In vivo imaging of cerebral microvascular plasticity from birth to death. J. Cereb. Blood Flow Metab. *33*, 146–156.

Hardie, D.G., Ross, F.A., and Hawley, S.A. (2012). AMPK: a nutrient and energy sensor that maintains energy homeostasis. Nat. Rev. Mol. Cell Biol. *13*, 251–262.

Harris, J.J., and Attwell, D. (2012). The energetics of CNS white matter. J. Neurosci. *32*, 356–371.

Hirose, K., Morita, M., Ema, M., Mimura, J., Hamada, H., Fujii, H., Saijo, Y., Gotoh, O., Sogawa, K., and Fujii-Kuriyama, Y. (1996). cDNA cloning and tissue-specific expression of a novel basic helix-loop-helix/PAS factor (Arnt2) with close sequence similarity to the aryl hydrocarbon receptor nuclear translocator (Arnt). Mol. Cell. Biol. *16*, 1706–1713.

Hu, F., and Strittmatter, S.M. (2004). Regulating axon growth within the postnatal central nervous system. Semin. Perinatol. *28*, 371–378.

Huang, S.M., Mishina, Y.M., Liu, S., Cheung, A., Stegmeier, F., Michaud, G.A., Charlat, O., Wiellette, E., Zhang, Y., Wiessner, S., et al. (2009). Tankyrase inhibition stabilizes axin and antagonizes Wnt signalling. Nature *461*, 614–620.

Huber, O., Korn, R., McLaughlin, J., Ohsugi, M., Herrmann, B.G., and Kemler, R. (1996). Nuclear localization of beta-catenin by interaction with transcription factor LEF-1. Mech. Dev. *59*, 3–10.

Ishibashi, T., Dakin, K.A., Stevens, B., Lee, P.R., Kozlov, S.V., Stewart, C.L., and Fields, R.D. (2006). Astrocytes promote myelination in response to electrical impulses. Neuron *49*, 823–832.

Ivan, M., Kondo, K., Yang, H., Kim, W., Valiando, J., Ohh, M., Salic, A., Asara, J.M., Lane, W.S., and Kaelin, W.G., Jr. (2001). HIFalpha targeted for VHL-mediated destruction by proline hydroxylation: implications for O2 sensing. Science *292*, 464–468.

Jaakkola, P., Mole, D.R., Tian, Y.M., Wilson, M.I., Gielbert, J., Gaskell, S.J., von Kriegsheim, A., Hebestreit, H.F., Mukherji, M., Schofield, C.J., et al. (2001). Targeting of HIF-alpha to the von Hippel-Lindau ubiquitylation complex by O2-regulated prolyl hydroxylation. Science *292*, 468–472.

Janzer, R.C., and Raff, M.C. (1987). Astrocytes induce blood-brain barrier properties in endothelial cells. Nature *325*, 253–257.

Jiang, L., Shen, F., Degos, V., Schonemann, M., Pleasure, S.J., Mellon, S.H., Young, W.L., and Su, H. (2011). Oligogenesis and oligodendrocyte progenitor maturation vary in different brain regions and partially correlate with local angiogenesis after ischemic stroke. Transl. Stroke Res. *2*, 366–375.

Joza, N., Pospisilik, J.A., Hangen, E., Hanada, T., Modjtahedi, N., Penninger, J.M., and Kroemer, G. (2009). AIF: not just an apoptosis-inducing factor. Ann. N Y Acad. Sci. *1171*, 2–11.

Kenney, A.M., Cole, M.D., and Rowitch, D.H. (2003). Nmyc upregulation by sonic hedgehog signaling promotes proliferation in developing cerebellar granule neuron precursors. Development *130*, 15–28.

Kinney, H.C., Brody, B.A., Kloman, A.S., and Gilles, F.H. (1988). Sequence of central nervous system myelination in human infancy. II. Patterns of myelination in autopsied infants. J. Neuropathol. Exp. Neurol. *47*, 217–234.

Kuhlmann, T., Miron, V., Cui, Q., Wegner, C., Antel, J., and Brück, W. (2008). Differentiation block of oligodendroglial progenitor cells as a cause for remyelination failure in chronic multiple sclerosis. Brain *131*, 1749–1758.

Lee, H., and Paik, S.G. (2006). Regulation of BNIP3 in normal and cancer cells. Mol. Cells *21*, 1–6.

Lee, Y., Morrison, B.M., Li, Y., Lengacher, S., Farah, M.H., Hoffman, P.N., Liu, Y., Tsingalia, A., Jin, L., Zhang, P.W., et al. (2012). Oligodendroglia metabolically support axons and contribute to neurodegeneration. Nature *487*, 443–448.

Liebner, S., Corada, M., Bangsow, T., Babbage, J., Taddei, A., Czupalla, C.J., Reis, M., Felici, A., Wolburg, H., Fruttiger, M., et al. (2008). Wnt/beta-catenin signaling controls development of the blood-brain barrier. J. Cell Biol. *183*, 409–417.

Lu, Q.R., Sun, T., Zhu, Z., Ma, N., Garcia, M., Stiles, C.D., and Rowitch, D.H. (2002). Common developmental requirement for Olig function indicates a motor neuron/oligodendrocyte connection. Cell *109*, 75–86.

Majmundar, A.J., Wong, W.J., and Simon, M.C. (2010). Hypoxia-inducible factors and the response to hypoxic stress. Mol. Cell *40*, 294–309.

Mazumdar, J., O'Brien, W.T., Johnson, R.S., LaManna, J.C., Chavez, J.C., Klein, P.S., and Simon, M.C. (2010). O2 regulates stem cells through Wnt/β-catenin signalling. Nat. Cell Biol. *12*, 1007–1013.

Ment, L.R., Schwartz, M., Makuch, R.W., and Stewart, W.B. (1998). Association of chronic sublethal hypoxia with ventriculomegaly in the developing rat brain. Brain Res. Dev. Brain Res. *111*, 197–203.

Miller, D.J., Duka, T., Stimpson, C.D., Schapiro, S.J., Baze, W.B., McArthur, M.J., Fobbs, A.J., Sousa, A.M., Sestan, N., Wildman, D.E., et al. (2012). Prolonged myelination in human neocortical evolution. Proc. Natl. Acad. Sci. USA *109*, 16480–16485.

Nave, K.A. (2010). Myelination and support of axonal integrity by glia. Nature *468*, 244–252.

Patel, S.A., and Simon, M.C. (2008). Biology of hypoxia-inducible factor-2alpha in development and disease. Cell Death Differ. *15*, 628–634.

Pham, L.D., Hayakawa, K., Seo, J.H., Nguyen, M.N., Som, A.T., Lee, B.J., Guo, S., Kim, K.W., Lo, E.H., and Arai, K. (2012). Crosstalk between oligodendrocytes and cerebral endothelium contributes to vascular remodeling after white matter injury. Glia *60*, 875–881.

Porfiri, E., Rubinfeld, B., Albert, I., Hovanes, K., Waterman, M., and Polakis, P. (1997). Induction of a beta-catenin-LEF-1 complex by wnt-1 and transforming mutants of beta-catenin. Oncogene *15*, 2833–2839.

Rankin, E.B., Higgins, D.F., Walisser, J.A., Johnson, R.S., Bradfield, C.A., and Haase, V.H. (2005). Inactivation of the arylhydrocarbon receptor nuclear translocator (Arnt) suppresses von Hippel-Lindau disease-associated vascular tumors in mice. Mol. Cell. Biol. *25*, 3163–3172.

Rinholm, J.E., Hamilton, N.B., Kessaris, N., Richardson, W.D., Bergersen, L.H., and Attwell, D. (2011). Regulation of oligodendrocyte development and myelination by glucose and lactate. J. Neurosci. *31*, 538–548.

Rosenstein, J.M., Krum, J.M., and Ruhrberg, C. (2010). VEGF in the nervous system. Organogenesis *6*, 107–114.

Ryan, H.E., Poloni, M., McNulty, W., Elson, D., Gassmann, M., Arbeit, J.M., and Johnson, R.S. (2000). Hypoxia-inducible factor-1alpha is a positive factor in solid tumor growth. Cancer Res. *60*, 4010–4015.

Sapieha, P. (2012). Eyeing central neurons in vascular growth and reparative angiogenesis. Blood *120*, 2182–2194.

Sawamiphak, S., Ritter, M., and Acker-Palmer, A. (2010). Preparation of retinal explant cultures to study ex vivo tip endothelial cell responses. Nat. Protoc. *5*, 1659–1665.

Semenza, G.L. (2012). Hypoxia-inducible factors in physiology and medicine. Cell *148*, 399–408.

Silbereis, J.C., Huang, E.J., Back, S.A., and Rowitch, D.H. (2010). Towards improved animal models of neonatal white matter injury associated with cerebral palsy. Dis. Model. Mech. *3*, 678–688.

Stenman, J.M., Rajagopal, J., Carroll, T.J., Ishibashi, M., McMahon, J., and McMahon, A.P. (2008). Canonical Wnt signaling regulates organ-specific assembly and differentiation of CNS vasculature. Science *322*, 1247–1250.

Stevens, B., Porta, S., Haak, L.L., Gallo, V., and Fields, R.D. (2002). Adenosine: a neuron-glial transmitter promoting myelination in the CNS in response to action potentials. Neuron *36*, 855–868.

Stolt, C.C., Schlierf, A., Lommes, P., Hillgärtner, S., Werner, T., Kosian, T., Sock, E., Kessaris, N., Richardson, W.D., Lefebvre, V., and Wegner, M. (2006). SoxD proteins influence multiple stages of oligodendrocyte development and modulate SoxE protein function. Dev. Cell *11*, 697–709.

Tan, S., Drobyshevsky, A., Jilling, T., Ji, X., Ullman, L.M., Englof, I., and Derrick, M. (2005). Model of cerebral palsy in the perinatal rabbit. J. Child Neurol. *20*, 972–979.

Tanaka, K., Nogawa, S., Ito, D., Suzuki, S., Dembo, T., Kosakai, A., and Fukuuchi, Y. (2001). Activation of NG2-positive oligodendrocyte progenitor cells during post-ischemic reperfusion in the rat brain. Neuroreport *12*, 2169–2174.

Tessitore, C., and Brunjes, P.C. (1988). A comparative study of myelination in precocial and altricial murid rodents. Brain Res. *471*, 139–147.

Wang, G.L., Jiang, B.H., Rue, E.A., and Semenza, G.L. (1995). Hypoxia-inducible factor 1 is a basic-helix-loop-helix-PAS heterodimer regulated by cellular O2 tension. Proc. Natl. Acad. Sci. USA *92*, 5510–5514.

Wang, Y., Rattner, A., Zhou, Y., Williams, J., Smallwood, P.M., and Nathans, J. (2012). Norrin/Frizzled4 signaling in retinal vascular development and blood brain barrier plasticity. Cell *151*, 1332–1344.

Weiss, J., Takizawa, B., McGee, A., Stewart, W.B., Zhang, H., Ment, L., Schwartz, M., and Strittmatter, S. (2004). Neonatal hypoxia suppresses oligodendrocyte Nogo-A and increases axonal sprouting in a rodent model for human prematurity. Exp. Neurol. *189*, 141–149.

Ye, F., Chen, Y., Hoang, T., Montgomery, R.L., Zhao, X.H., Bu, H., Hu, T., Taketo, M.M., van Es, J.H., Clevers, H., et al. (2009a). HDAC1 and HDAC2 regulate oligodendrocyte differentiation by disrupting the beta-catenin-TCF interaction. Nat. Neurosci. *12*, 829–838.

Ye, X., Wang, Y., Cahill, H., Yu, M., Badea, T.C., Smallwood, P.M., Peachey, N.S., and Nathans, J. (2009b). Norrin, frizzled-4, and Lrp5 signaling in endothelial cells controls a genetic program for retinal vascularization. Cell *139*, 285–298.

Yuen, T.J., Johnson, K.R., Miron, V.E., Zhao, C., Quandt, J., Harrisingh, M.C., Swire, M., Williams, A., McFarland, H.F., Franklin, R.J., and Ffrench-Constant, C. (2013). Identification of endothelin 2 as an inflammatory factor that promotes central nervous system remyelination. Brain *136*, 1035–1047.